PII: S0032-3861(97)10026-X

Polymer Vol. 39 No. 14, pp. 3017–3027, 1998

0032-3861/98/$19.00+0.00

The effect of extensional flow on the Raman spectra of dilute polymer solutions

S.D. Cooper, D.N. Batchelder* and P. Ramalingam†
Department of Physics and Astronomy, University of Leeds, Leeds LS2 9JT, UK
(Received 27 June 1997)

Raman spectroscopy has been used to investigate the dynamics of the coil-stretch transition of dilute polymer solutions. A stagnation-point extensional-flow field was created by an opposed jets apparatus. High molecular weight, closely monodispersed *cis*-polyisoprene was studied in 1,1,1-trichloroethane, a good solvent for this polymer. Raman spectra were obtained with a spatial resolution of 10 (μm in the extensional flow region. The vibrational frequency of the ν(C = C) stretch at 1664 cm^{-1} was shown to be sensitive to the strain rate of the extensional flow field. No changes were observed in the Raman spectra until the strain rate was larger than the critical value for the coil-stretch transition. The Raman band was then observed to shift linearly to lower frequency with increasing strain rate before saturating. The observed changes were much smaller, however, than those predicted using a model of a fully extended chain in the flow field.

(Keywords: Raman; extensional flow; polymer solutions)

INTRODUCTION

Polymer chains in a dilute solution can be readily deformed by an extensional flow field. There is a considerable body of evidence to show that it is possible, under appropriate conditions, to realise the full coil-stretch transition for monodispersed solutions once a critical strain rate has been exceeded[1]. At higher strain rates it has even proved possible to fracture the polymer chains[2]. These dramatic changes in polymer structure should cause significant changes in Raman spectra recorded from scattering volumes within the extensional flow field.

The velocity gradient in a flow field can be described by a tensor which can be split into two parts: the elongational component which acts to extend a fluid element and the rotational component which does not significantly deform coiled polymer molecules in solution. Little chain deformation takes place in simple shear flows as the extensional and rotational parts are equal. If the elongational component of the flow dominates, however, this acts to extend the molecules. A persistently extensional flow field is necessary to extend polymer coils in solution; this can be achieved if the elongational component is greater than the rotational and the molecules spend sufficient time in the flow field[3,4].

Extensional flow fields can be created in several ways; successful techniques include opposed jets, rotating mills and crossed slots[1]. The most appropriate system for use in Raman experiments is the opposed jets; higher strain-rate flow fields can be generated than with the rotating mill and the region of extensional flow is optically more accessible for spectroscopy than with crossed slots. Several different polymers have been investigated but the most widely studied are polystyrene and poly(ethylene oxide)[1,5]. Two recent studies based on these materials have provided considerably more detail about the molecular behaviour in extensional flow. Extensive analysis of the spatial distribution of molecular orientation in the region of extensional flow has been made as a function of concentration[6,7] and a detailed comparison has been made of the differences between transient and stagnation point elongational flows[8,9].

The primary technique used for studying the response of polymer molecules to an extensional flow has been optical birefringence. When polymer molecules are aligned by the flow field, the refractive indices for light polarised parallel and perpendicular to the alignment directions are different. Birefringence of the solution is observed for polymer molecules under these conditions; a measure of the birefringence is the difference in refractive index, Δn, between light polarised parallel and perpendicular to the elongation axis. When observed between crossed polarisers, a narrow birefringent line appears in dilute solutions of flexible polymers at the onset of molecular extension, along the centre symmetry line between the jets. The intensity of light transmitted between crossed polarisers is proportional to $(\Delta n)^2$.

The strain rate $\dot{\epsilon}$ in the opposed jets apparatus may be approximated as

$$\dot{\epsilon} = \frac{Q}{\pi r^2 d} \tag{1}$$

where Q is the volumetric flow rate, r is the radius and d is the distance between the jets[1,2,10]. For a monodisperse polymer solution there is a sudden increase in the birefringence at a critical strain rate, $\dot{\epsilon}_c$, that is indicative of the chains suddenly extending. For a chain to extend, the extensional forces on the chain have to overcome the forces trying to restore the molecule to its original unperturbed state. These extensional forces are transmitted through frictional forces between fluid and chain.

The behaviour of polymer coils in an extensional flow field has been modelled using several different approaches. For example, Zimm[11] used a bead-spring model with a chain of beads connected by Hookean springs. He included the hydrodynamic interaction between polymer and solvent where one bead screens another from the flow. De Gennes[12]

* To whom correspondence should be addressed
† Current address: Physics Department, Universiti Brunei Darussalam, Bandar Seri Begawan 2028, Negara Brunei Darussalam

showed that a polymer coil should unwind abruptly when the critical velocity gradient is reached. As the coil begins to unwind more of the segments become exposed to the flow enhancing the chain extending effect and exposing still more segments. Recently, various models for computer simulation of polymer chains have been developed. The Brownian dynamics technique[13] and the Monte Carlo approach[14] have been applied to a model for a polymer chain consisting of beads connected by springs.

The disadvantage of using birefringence measurements to measure chain extension is the lack of spatial resolution; contributions are made over the whole path length through the extensional flow region. Assumptions have to be made about the symmetry of the flow field and a deconvolution procedure carried out to calculate the birefringence at each point[6,15]. Raman spectroscopy is a more informative way of studying polymer molecules in solution as the scattering volume involved can be selected. The orientation of the molecules can be determined and, in addition, Raman spectra are very sensitive to slight changes in local structure such as changes in bond length and bond angle[16]. Strain produced in a molecule by an extensional flow field should have the greatest effect on molecular vibrations involving motion of the atoms on the polymer backbone. Indeed, part of the original motivation for these experiments was the possibility of determining the interatomic force constants on a polymer backbone at stresses sufficiently high for chain scission to be induced by the extensional flow[4]. One drawback of the application of the technique to dilute solutions is that a careful choice of solvent has to be made or the Raman bands from the polymer will not be visible. We believe that this is the first attempt to use Raman spectroscopy in extensional flow experiments.

EXPERIMENTAL SECTION

The extensional flow field was produced by a system of opposed, cylindrical glass jets through which the polymer solutions were sucked. The jets consisted of two glass capillaries of 0.48 mm internal diameter arranged so that the capillaries faced each other with a gap of 0.61 mm between them. This arrangement created a stagnation point on the symmetry line between the jets; polymer molecules that passed along streamlines close to this point experienced a uniaxial extensional force. The jets were connected via a series of reservoirs to a diaphragm pump that circulated the solution through the system. The flow cell containing the jets was constructed from stainless steel with Spectrosil glass windows and is shown schematically in *Figure 1*. The 514.5 nm line from an argon laser (Cambridge Lasers Model CL-4W) was used as the excitation source. The laser beam was first passed through a monochromator to remove plasma lines, then through a beam expander with spatial filter to clean the beam and make a sharper focus possible. A 20X Olympus MSPlan ultra-long working distance microscope objective was used to focus the beam into the flow cell.

The Raman scattered light was collected at 90° by an f/1.2, 50 mm camera lens (Pentax) and focused by a second lens onto the entrance slit of a 0.85 m double monochromator (SPEX 1401). The intensity of the Rayleigh scattered light entering the spectrometer was first reduced by a holographic rejection filter (Kaiser). A liquid nitrogen cooled CCD system supplied by Wright Instruments was used as the detector. The 400 by 592 pixels of the EEV P8603 CCD chip were 22.5 μm square. A test image was used to calibrate the spatial resolution of the CCD; each pixel on the CCD was found to represent a vertical distance of 2.9 ± 0.2 μm in the flow cell. A polarisation scrambler was also inserted in the optical path for depolarisation measurements of the Raman scattered light.

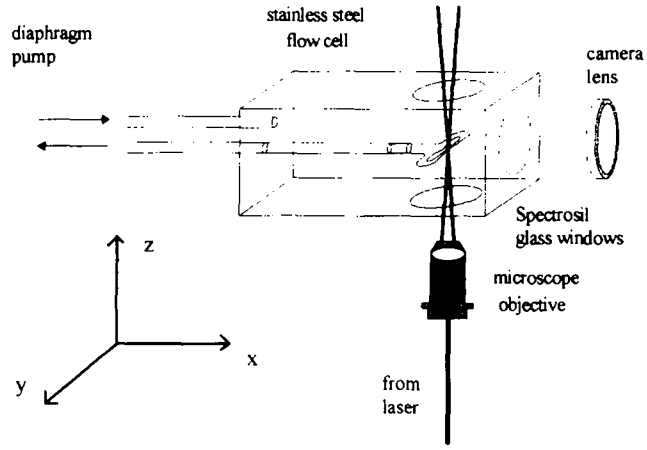

Figure 1 Schematic diagram of the extensional flow cell. The laser beam is travelling in the z-direction, the glass capillary tubes are aligned along the y-axis and the scattered light is collected in the x-direction

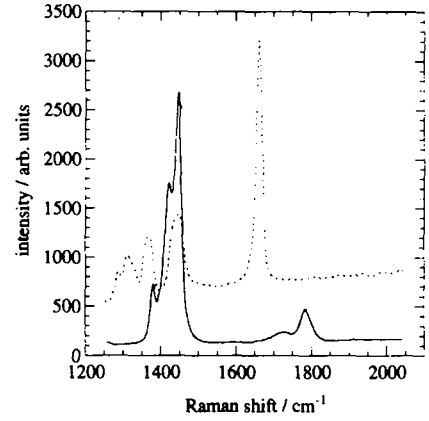

Figure 2 Comparison of the Raman spectra of solute and solvent. The dashed line is the spectrum of *cis*-polyisoprene powder (integration time 1 s) and the solid line is 1,1,1-trichloroethane (integration time 5 s)

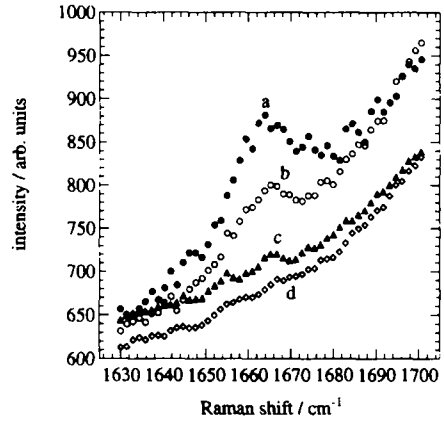

Figure 3 Raman spectra of solutions of *cis*-polyisoprene in 1,1,1-trichloroethane spectra were recorded in 30 s with the following concentrations: (a) 0.1%, (b) 0.03%, (c) 0.01%, (d) 0.005%

Choice of materials

The polymers used in the extensional flow experiments

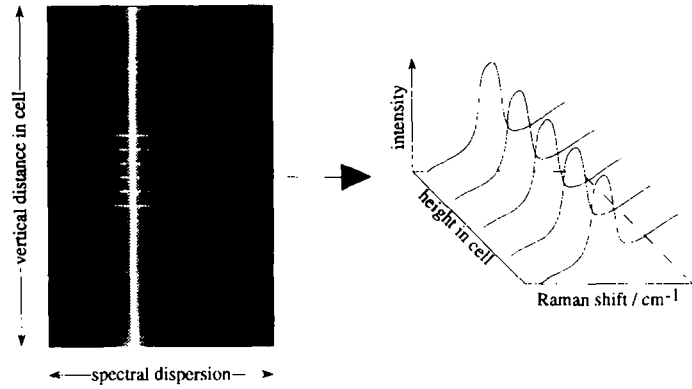

Figure 4 Schematic diagram of the two-dimensional output of the CCD showing the selected area (solid lines) and, for example, five separately binned regions within it (dashed lines). The five spectra from the binned regions are shown dispersed horizontally across the CCD; the binned regions at different vertical heights on the CCD correspond to different positions along the z-axis in the cell (see *Figure 1*)

needed to be of high molecular weight so that the strain rates required to extend them were accessible by the apparatus. Several different combinations of polymer and solvent were tested for suitability with these experiments. *Cis*-polyisoprene (cPI) was finally chosen for these experiments as it is a highly flexible molecule, has carbon double bonds in its backbone and has previously been investigated in extensional flow experiments[17]. The Raman band for the double-bond, symmetric-stretch vibration ν(C=C) at 1664 cm^{-1} is intense and well separated from all the other bands in the Raman spectra of the polymer[18]. The double bonds are approximately parallel to the backbone of the extended polymer molecule so that the Raman band frequency should have maximum strain sensitivity.

The solvent was chosen to be 1,1,1-trichloroethane as it has a moderately high viscosity compared to other possible solvents and has no first-order Raman bands in the spectral region of interest. *Figure 2* compares the Raman spectra of solid cPI and 1,1,1-trichloroethane. In the long integration times necessary for observing the solute bands in dilute solutions, several high-order bands from the solvent become visible in the spectra. These bands were investigated using polarised Raman measurements and were found to arise from combination bands of the fundamental vibrations. These weak solvent bands are stronger than the first-order Raman bands of cPI at the low concentrations used and give a sloping background to the spectrum of the ν(C=C) band. As shown in *Figure 3*, this band can be detected in solution down to concentrations as low as 0.01% by weight of solute in solvent; this limit arises from the noise associated with the Raman signal of the combination band.

Preparation

All the polymer solutions were prepared by dissolving cPI (Polymer Laboratories) in 1,1,1-trichloroethane (BDH). The cPI used for most of the experiments had an average molecular weight of 4.4×10^6 with a polydispersity factor M_w/M_n of 1.18; unless specifically stated otherwise, this is the molecular weight of the material used in the experiments described in this paper. The units of concentration are mass/volume: 1% describes a solution in which 1 g of polymer has been dissolved in 100 ml of solvent. The solvent was used as supplied and the cPI was added in a sealed flask. The solution was left, with occasional stirring, for one week to ensure complete dissolution. Prior to use, the solution was filtered through a 40 μm pore size sintered glass funnel to remove particulates. Experiments were also carried out with cPI of molecular weights 1.2×10^6 and 2.65×10^6, both with $M_w/M_n = 1.03$.

The intrinsic viscosity of the 4.4×10^6 M_w solution was found to be 9.83 dl g^{-1} using an Ubbelohde viscometer. The critical concentration for coil overlap, c*, for this system was thus calculated to be approximately 0.1%[19]. Comparison with values for other solvents suggests that 1,1,1-trichloroethane is a 'good' solvent for cPI[20]; explicit data for this system do not appear to exist.

Extensional flow experiments

Raman spectra were recorded with a laser power of 300 mW and data collection times of 300–600 s. The beam waist of the laser at the position of focus was measured, using the CCD, to be about 10 μm in diameter and the extensional flow region was found to have a diameter of approximately 100 μm. The fixed grating position in the spectrometer produced a spectral range of approximately 100 cm^{-1} and a dispersion of 0.35 cm^{-1} per pixel at the CCD, both sufficient for these experiments. With Lorentzian curves fitted to the data, shifts in the peak position could be measured with a relative accuracy of 0.05 cm^{-1}. The temporal stability of the spectrometer was confirmed by measuring the position of the 520 cm^{-1} Raman band of silicon; in 10 h the position deviated by less than 0.05 cm^{-1}.

Optical absorption measurements for a 0.21% solution of 4.4×10^6 M_w cPI in 1,1,1-trichloroethane indicated that less than 1% of the laser beam was absorbed in traversing the 10 mm diameter cell; the fraction actually absorbed would almost certainly be considerably less than this. A rough estimate suggested that the laser beam would cause a temperature rise in the non-flowing solution of less than 2 K above the ambient temperature of 295 K, even at the region of best focus which was approximately 10 μm in diameter. No bubbles were ever formed along the path of the laser beam in the solutions which had a boiling point of 347 K, thus giving an absolute limit to the possible temperature rise. In addition, halving the intensity of the laser produced no detectable changes in the observed Raman spectra.

The location of the flow cell relative to the laser beam and the collection optics was controlled by an *xyz* micrometer stage to $\pm$ 2 μm. Crude positioning of the cell was carried out by observing the birefringence of the transmitted laser beam, which had to be attenuated for the measurement. The enhanced intensity of the Rayleigh scattered light in the region of extensional flow was used to make fine adjustments of position.

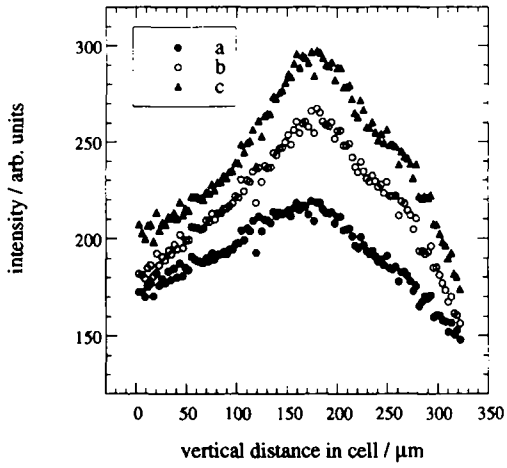

Figure 5 The variation in intensity of the Rayleigh scattered light along the z-axis (see *Figure 1*) through the centre of the extensional flow region as measured by the CCD for a 0.087% solution of 4.4×10^6 M_w *cis*-polyisoprene. The centre of the region of extensional flow is at about $z = 175$ μm. The magnitudes of the strain rate, $\dot{\epsilon}$, were: curve (a), 4920 s^{-1}; curve (b), 6950 s^{-1}; curve (c), 8110 s^{-1}. The curves have been displaced vertically for clarity

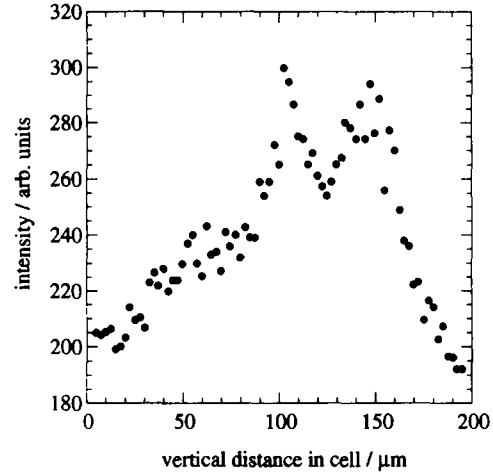

Figure 6 The variation in intensity of the Rayleigh scattered light along the z-axis (see *Figure 1*) through the centre of the extensional flow region as measured by the CCD for a 0.06% solution of 4.4×10^6 M_w *cis*-polyisoprene. The centre of the region of extensional flow is at about $z = 125$ μm and the strain rate, $\dot{\epsilon}$, was 14 000 s^{-1}

The CCD controlling software was used to record scattered light only from the region of interest in the flow cell in order to speed data processing. The 2D rectangular area on the CCD corresponding to the extensional flow region is shown schematically in Figure 4. The bright, vertical band represents the Raman scattered light excited by the laser beam as it traverses the cell. The columns of CCD pixels represent vertical distance in the flow cell with the rows representing spectral dispersion. The pixel height on the CCD was equivalent to a 2.9 ± 0.2 μm vertical distance in the flow cell. Pixels in the vertical direction can be binned together to increase the signal or to give the average spectrum over a region. Although binning the data reduces the spatial resolution in the cell, it has the benefit of reducing the noise level; usually the signals from two rows of pixels were added together. Raman spectra simultaneously taken at different vertical heights in the extensional flow region were then extracted from this data as shown schematically in *Figure 4*. These spectra were analysed and compared to give information on the changes occurring in the flow field. Maps of the Raman spectra within the 3D volume of extensional flow were recorded by translating the cell in the x, y plane.

The Raman spectra were fitted to Lorentzian curves using a non-linear least squares Levenburg-Marquardt routine[21], after first subtracting a quadratic background. The peak position, intensity, and width were determined for the spectra from each row of pixels. The results from this fitting were loaded into a spreadsheet program where graphical representations of the peak position data were produced. The regions where changes had occurred in the flow were, thus, highlighted so that they could be analysed in more detail.

RESULTS AND DISCUSSION

A number of features in the present experiments are analogous to the recent results of Carrington *et al.*[6]; these authors made spatially resolved birefringence measurements of atactic polystyrene and polyethylene oxide solutions over a wide concentration range. These are different systems to the one studied here but there should be strong qualitative similarities. At the lowest concentrations, below c*/10, the authors found a well-behaved, localised birefringence. For example, as the strain rate of a 0.01% $M_p = 4 \times 10^6$ aPS/decalin solution increased above $\dot{\epsilon}_c$, the radial dependence of the birefringence profile remained approximately Gaussian in shape with a gradually increasing width. The maximum birefringence was located on the flow axis; with increasing flow rate above $\dot{\epsilon}_c$, the birefringence maximum followed a sigmoidal dependence to a plateau value that was in rough agreement with theoretical predictions.

At higher concentrations, the authors[6] observed effects which they attribute to screening of molecules by their neighbours. For example, as the strain rate of a 0.02% $M_p = 8 \times 10^6$ aPS/decalin solution increased above $\dot{\epsilon}_c$, the birefringence was initially well behaved. Above a critical value of the strain rate $\dot{\epsilon}_s$, however, the birefringence saturated and the radial dependence of the birefringence profile split into two peaks with a minimum in the birefringence located on the flow axis. The saturation value of the birefringence was well below that predicted by theory. It is believed that the dynamic behaviour of polymer molecules at some distance from the axis of flow was distorting the flow field for molecules on and near the axis.

It is likely that the polymer solutions studied here were in a similar concentration range to the latter example of Carrington *et al.*[6] that showed screening effects. Thus, it is possible to interpret some of the observations in the present experiments in a similar way.

Rayleigh scattering

Rayleigh scattering of polymer solutions is often used to determine the molecular weight and radius of gyration of the polymer molecules. This was not possible in the present experiments as the scattering angle was fixed at 90°. In this geometry, however, enhanced Rayleigh scattering was observed in the region of extensional flow, in agreement with previous observations in solutions of hydrolysed polyacrylamide[22]. The Rayleigh scattering was stronger than the Raman, even after passing through the holographic rejection filter, and was of considerable assistance in defining the region of extensional flow. The filter was left in place for the Rayleigh scattering measurements in order

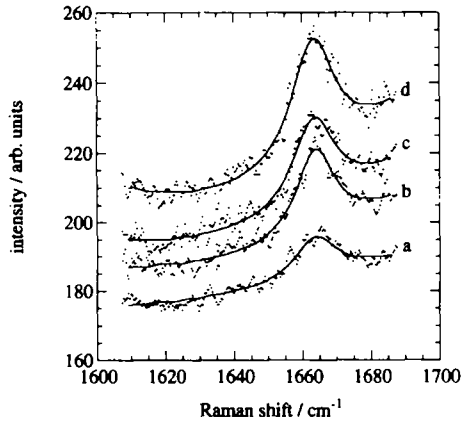

Figure 7 The raw data and the fitted Lorentzian curves for a 0.087% solution of 4.4 × 10^6 M_w *cis*-polyisoprene; the dots represent the raw data and the solid lines the fitted curves: (a) $\dot{\epsilon} = 0$ s^{-1}; (b) $\dot{\epsilon} = 3800$ s^{-1}; (c) $\dot{\epsilon} = 4500$ s^{-1}; (d) $\dot{\epsilon} = 5300$ s^{-1}

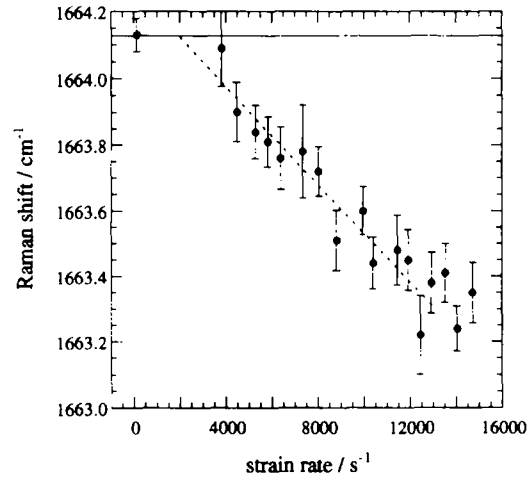

Figure 8 The Raman frequency of the ν(C=C) vibration of a 0.05% solution of 4.4 × 10^6 M_w *cis*-polyisoprene as a function of strain rate, $\dot{\epsilon}$. The values have been averaged over the region of extensional flow (29 pixels on the CCD, corresponding to a height of 85 μm in the flow cell). The solid line shows the frequency at zero flow

to maintain the optical alignment of the system. *Figure 5* shows the intensity of the Rayleigh scattered light in a vertical line through the extensional flow region for the 0.087% solution for three different strain rates. The intensity of the Rayleigh scattered light from the extensional flow region is clearly greater than that from outside that region. The double bond is the most polarisable unit in cPI; when this bond is aligned in the extensional flow direction, also the direction of the laser polarisation, then enhanced Rayleigh scattering is expected. The boundaries of the region of extensional flow are not sharp, as found from spatially resolved birefringence measurements[6]. The full-width at half maximum for the region of Rayleigh scattering enhancement is approximately 100 μm.

The results of *Figure 5* show a continuing enhancement of the Rayleigh scattering with increasing extensional flow rate; the shape is roughly Gaussian. This result is in agreement with the only detailed study of Rayleigh scattering under conditions of extensional flow[23]. Evidence for molecular screening in the present experiments was observed at higher strain rates; *Figure 6* shows a double peak in the Rayleigh scattering of a 0.06% solution of cPI at a strain rate of 14 000 s^{-1}. The profile is very similar to that observed by Carrington *et al.*[6] for the birefringence, above the saturation value $\dot{\epsilon}_S$ for the strain rate, of the 0.02% M_p = 8 × 10^6 aPS/decalin solution.

Dependence of the Raman frequency on strain rate

A typical series of Raman spectra are shown in *Figure 7* for a 0.087% cPI solution. The scattering volume sampled was approximately 500 μm^3 and the integration times were 400 s. The spectra show both the raw data obtained and the fitted Lorentzian curves; for clarity the curves have been displaced along the intensity axis. The intensity of the Raman spectra were observed to increase with increasing strain rate and a slight shift of the peak position to lower frequencies was noted. This increase in Raman intensity is expected for greater alignment of the C=C bonds with the collinear axes of extensional flow and laser polarisation. Thorough investigation showed that no statistically significant changes were observed in the width of the Raman band with increasing strain rate.

In Raman terms, the region of extensional flow was defined by the upper and lower rows of pixels where the Raman band showed a statistically significant frequency shift. The size of the region exhibiting strain was found to depend upon the concentration of the solution. For a 0.05% solution the region was found to be approximately 85 μm across whereas for the 0.087% solution the diameter was 145 μm, at similar values of $\dot{\epsilon}$. Analogous concentration effects were observed by Carrington *et al.* in their birefringence studies[6].

The average peak position of the Raman band within the region of extensional flow region is plotted against strain rate for the 0.05% solution in *Figure 8*. The error bars are the standard deviation in the fitted peak position over the region. There are three distinct regions in the data. The frequency of the Raman band remains constant until the strain rate exceeds the critical value $\dot{\epsilon}_c$; then the Raman frequency $\bar{\nu}$ decreases linearly with increasing $\dot{\epsilon}$. Finally, the Raman frequency remains constant above a saturation strain rate $\dot{\epsilon}_s$. Similar behaviour is seen more clearly for 0.087% concentration in *Figure 9*; in addition the gradient $\partial\bar{\nu}/\partial\dot{\epsilon}$ of the linear region is increased and $\dot{\epsilon}_s$ is lower.

In *Figure 9* comparison is also made between the average frequency of the Raman band over the whole 140 μm region of extensional flow and the maximum shifted value taken from two rows of pixels from the CCD, corresponding to an average over a height in the cell of 5.8 μm. The gradient of the fitted line to the 5.8 μm diameter data is larger than that of the 140 μm data while both $\dot{\epsilon}_c$ and $\dot{\epsilon}_s$ are reduced. This clearly demonstrates the non-uniformity of the region of extensional flow and is in accordance with other results that show that, below $\dot{\epsilon}_s$, the strain-rate is greatest on the flow axis.

The clear presence of the saturation effect in all the solutions studied here is strong evidence that concentrations used were in the region where screening effects are important. It is noticeable, however, that both the present data and the data of Carrington *et al.*[6] show behaviour approximating that of a dilute solution at strain rates below $\dot{\epsilon}_s$.

Depolarisation ratio

There is some uncertainty about the symmetry properties of cPI. In the amorphous solid, which should have similar molecular orientational properties to the unperturbed solution, it has been suggested that the symmetry of the cPI chain is either C_1 or C_S, while the aligned chains are

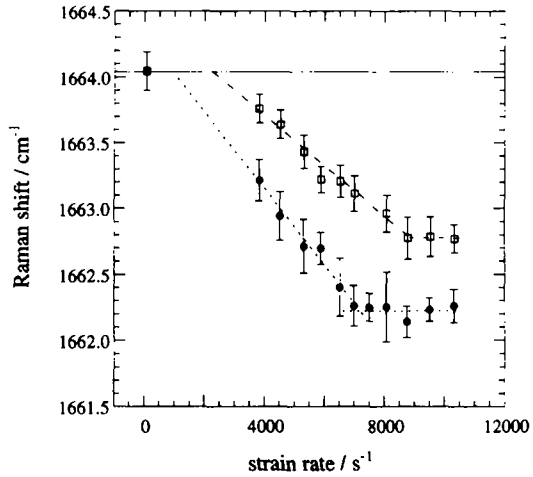

Figure 9 The Raman frequency of the ν(C=C) vibration of a 0.087% solution of 4.4 × 10^6 M_w *cis*-polyisoprene as a function of strain rate, $\dot{\epsilon}$: squares, average of the frequency over the region of extensional flow (48 pixels, corresponding to 140 μm); circles, frequency values at the centre of the region of extensional flow (2 pixels, corresponding to 5.8 μm)

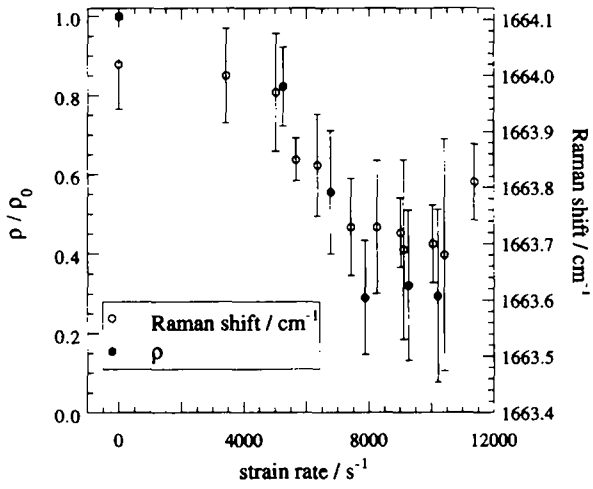

Figure 10 Comparison of the Raman frequency and the relative depolarisation ratio of the ν(C=C) vibration for a 0.21% solution of 4.4 × 10^6 M_w *cis*-polyisoprene as a function of strain rate, $\dot{\epsilon}$

suggested to have C_S symmetry[18,24]. In the latter case, with the laser polarised parallel to the polymer chain, we expect the depolarisation ratio of the ν(C=C) vibration to be close to zero. Values of ρ were determined for a 0.21% semi-dilute solution of 4.4 × 10^6 M_w cPI. A high concentration was used in order to obtain statistically significant value for ρ. In the unperturbed solution ρ was found to be 0.12 ± 0.01. *Figure 10* compares ρ with the Raman frequency as a function of strain rate in the region of extensional flow. The depolarisation ratio follows the Raman frequency, even saturating at the same strain rate. The saturation value ρ_s was found to be 0.04 ± 0.01; this finite value suggests that, although there has been a considerable degree of chain segment alignment, not all the polymer has become fully aligned in the direction of extensional flow before saturation is reached. This result is in qualitative agreement with the birefringence results Carrington *et al.*[6] for solutions in which screening was observed. *Figure 10* also illustrates that, with the concentration greater than c^*, the gap between $\dot{\epsilon}_c$ and $\dot{\epsilon}_s$ has become very narrow.

Spatial variation of the Raman frequency

Experiments were performed to investigate the spatial

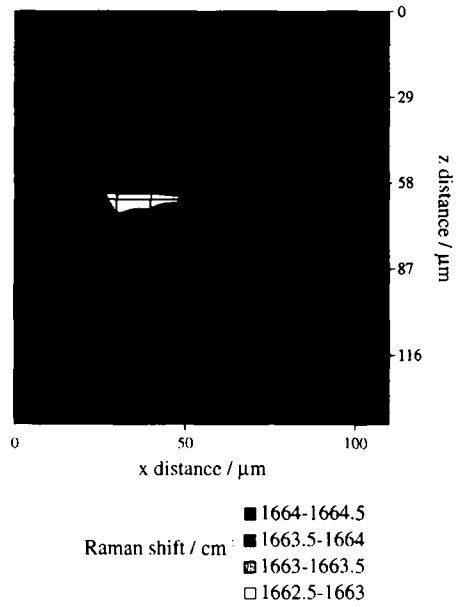

Figure 11 The frequency of the ν(C=C) Raman band at different points in the *xz* plane (a section perpendicular to the flow) for a 0.05% solution of 4.4 × 10^6 M_w *cis*-polyisoprene at a strain rate of 7160 s^{-1}

variation of the Raman frequency throughout the region between the jets. The cell was moved along the *x* axis, the direction of scattered light collection, between each successive spectrum. Each CCD exposure taken consists of a series of spectra at different heights in the flow cell. Thus, when the position of the laser focus is changed by moving the flow cell, a series of spectra at different heights at a new *x* position is produced (see *Figure 1*). By this method a 'map' of the Raman frequency shift of the ν(C=C) vibration can be created for the *x*, *z* plane.

Figure 11 shows a map in the *x*, *z* plane that contains the stagnation point for a 0.05% cPI solution at a strain rate of 7160 s^{-1} (below $\dot{\epsilon}_s$). The different shaded regions show the position of the ν(C=C) line at each point on the *x*, *z* plane. The unshifted regions are shaded in dark grey, and the regions that show a slight frequency shift are shaded light grey. The region that exhibits the largest shifts is shaded white. An area of large shifts of approximately circular shape and diameter 30 μm, can be observed to the left of centre in *Figure 11*; we believe that this region contains the stagnation point. The reproducibility of the changes in the Raman frequency were investigated for the same solution at an identical strain rate, after switching all the equipment off, then on again, and realigning the system. The location of the identified stagnation point remained the same.

Semi-dilute solutions, $c > c^*$, of cPI were also studied, as the behaviour in flow of these solutions is expected to be different from the dilute solutions studied previously. The higher polymer concentration makes the solution more viscous, so the critical strain rate will occur at lower value. Network effects are also expected to occur and may extend over a large volume. The solution investigated was a 0.225% solution of 1.2 × 10^6 molecular weight cPI; this solution had a calculated critical strain rate of 5500 s^{-1}. The vibrational frequency was measured at different points in the *x*, *z* plane for $\dot{\epsilon} = 7460$ s^{-1} and the results are shown in *Figure 12*. The region of highest strain is shaded white and the region exhibiting slight changes is shaded in grey. A region of small frequency change in the centre of a region of large change can be clearly observed, strong evidence for a 'pipe' structure[25]; the stagnation point is believed to be

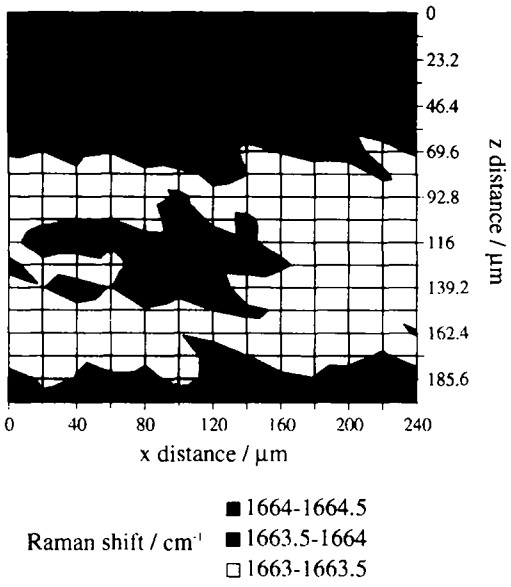

Figure 12 Frequency of the ν(C=C) Raman band at different points in the xz plane (a section perpendicular to the flow) for a 0.225% solution of 1.2×10^6 M_w *cis*-polyisoprene at a strain rate of 7460 s^{-1}

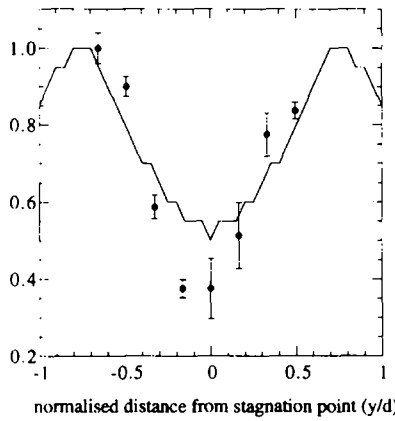

Figure 13 Comparison of the measured frequency shift (relative to the maximum value of 0.80 cm^{-1}) of the ν(C=C) Raman band with the calculated magnitude of the strain rate, $\dot{\epsilon}$, (relative to the maximum value) as a function of position along the y-axis. The Raman measurements were taken of a 0.05% solution of 4.4×10^6 M_w *cis*-polyisoprene with a nominal strain rate of 7162 s^{-1}. The potential flow calculation was carried out by Carrington *et al.*[6] for a flow geometry similar to that in the present experiments

located in this region. It is probable that both screening and entanglement effects are important at this high concentration.

The variation of Raman frequency of the ν(C=C) band along the centre of the extensional flow region between the jets (i.e. along the y axis, see *Figure 1*) was also measured for a 0.05% solution of 4.4×10^6 M_w cPI at a nominal strain rate of 7162 s^{-1}. In *Figure 13* the Raman frequency shift data, relative to the maximum observed value of 0.80 cm^{-1}, are plotted as a function of the normalised distance from the centre of the jets. The frequency shift near the jet orifice is more than three times that at the centre. Also plotted as the solid line in *Figure 13* is the result of a potential flow calculation for jets with a similar geometry to those used in the present experiments[7]. There is good agreement between the shift in the Raman frequency, which is expected to be proportional to strain rate (see below), and the theoretical model.

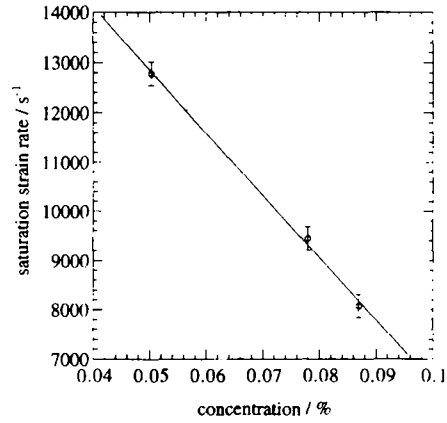

Figure 14 The saturation strain rate, $\dot{\epsilon}_s$, for the frequency of the ν(C=C) Raman band as a function of concentration for solutions of 4.4×10^6 M_w *cis*-polyisoprene in 1,1,1-trichloroethane. The straight line represents a least-squares fit to the data

Concentration dependence

The results presented thus far demonstrate the importance of screening effects in the properties under study. As the solutions investigated here have concentrations approaching the minimum required for molecular overlap, it is possible that molecular entanglements may also occur. Both screening and molecular entanglements cause changes in the flow field that have been observed by changes in birefringence patterns, e.g. 'pipes'[25]. Screening is believed to be caused by extending molecules that extract energy from the flow field so that the strain supplied by the fluid will no longer be sufficient to maintain molecular extension[26]. When molecular entanglements occur, the subsequent formation of molecular networks is expected to cause severe disruption of the flow field.

Figure 14 provides evidence that the saturation of $\partial\bar{\nu}/\partial\dot{\epsilon}$, as seen for example in *Figure 9*, is likely to be a result of screening, rather than molecular entanglements. Screening effects should scale as a relatively simple function of the concentration while entanglements effects can be expected to depend in a very non-linear manner with concentration. The value of $\dot{\epsilon}_s$ decreases linearly with concentration in *Figure 14*, as might be expected if this were a screening phenomenon. Furthermore, the double peak observed in the Rayleigh scattering in *Figure 6* at a high strain rate suggests that the saturation of $\partial\bar{\nu}/\partial\dot{\epsilon}$ and the formation of 'pipes', evidence for screening as well as entanglements, are correlated.

As shown below for a simple model, the decrease of Raman frequency with strain rate is expected to be proportional to viscosity. In *Figure 15*, the magnitude of the strain rate dependence of the Raman frequency, $\partial\bar{\nu}/\partial\dot{\epsilon}$, averaged over the extensional flow region, e.g. the slopes in *Figures 8 and 9*, is plotted as a function of viscosity. The lower two concentrations lie on a straight line through the origin while the value for the highest concentration is approximately a factor of two above this line. *Figure 15* provides substantial evidence that, at least at strain rates below $\dot{\epsilon}_s$, molecular entanglements only become important at concentrations above 0.078%. At this and the lower concentrations studied, we believe that the results presented here are largely representative of the behaviour of solutions in which only screening effects perturb the flow field.

Degradation study

Degradation of the cPI molecules during an experiment should lead to a rapid decrease in the shift in the Raman

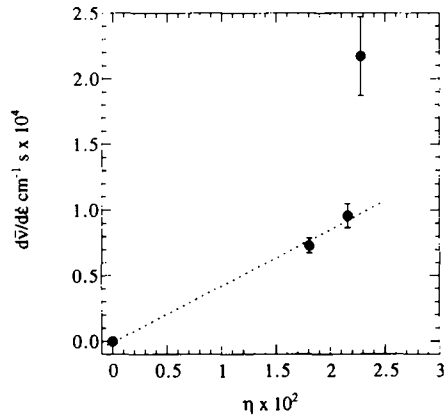

Figure 15 Plot of slope of Raman shift, $\frac{d\nu}{d\dot{\epsilon}}$, averaged over the extensional flow region (see *Figures 8 and 9*) as a function of the viscosity of the solution. The three data points correspond, with increasing viscosity, to 0.05%, 0.078% and 0.087% solutions of 4.4×10^6 M_w *cis*-polyisoprene in 1,1,1-trichloroethane

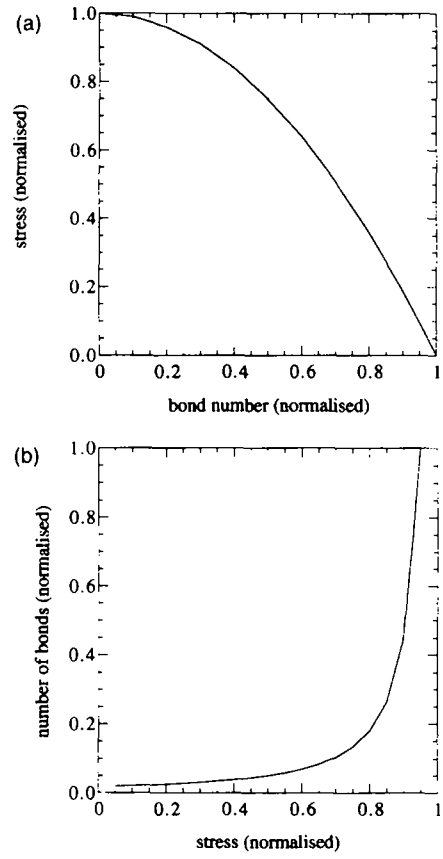

Figure 16 Stress distribution along an extended polymer molecule in an extensional flow field calculated using the bead-rod model: (a) the distribution of stress, normalised to unity, along the bonds of a polymer chain; (b) the number of bonds in each stress interval in (a)

frequency. There are two reasons for this. At constant viscosity, the broken molecules will experience a smaller extensional stress owing to the fact that they are shorter. The degradation will, however, also reduce the viscosity of the solution and thus cause further reduction in the Raman shift induced by the extensional flow field. Hence, during extensional flow, we expect the Raman frequency to be very sensitive to the onset of degradation.

A test of degradation effects was carried out on a 0.065% solution of 4.4×10^6 M_w cPI. The solution was left circulating through the system at a constant strain rate of $\dot{\epsilon} = 13590\ s^{-1}$; the strain rate for molecular fracture was estimated using equation (6) to be about $13000\ s^{-1}$. At intervals the strain rate was lowered to $\dot{\epsilon} = 9513\ s^{-1}$ and the Raman spectrum recorded. The experiment was run for more than 7 h before a statistically significant reduction was observed in the shift of the Raman frequency; this was equivalent to more than 100 passes of the solution through the cell. We conclude that chain scission is a relatively rare event under the present experimental conditions.

Strain rate dependence of the Raman frequency: a simple model

The Raman data presented in this paper demonstrate that the frequency of the C=C bond is dependent upon the strain rate experienced by the molecule in the extensional flow field. The functional dependence and magnitude of this effect can be predicted through the application of a simple model.

Calculation of the shift in the Raman frequency of a vibrational mode depends on knowledge of how the molecular conformation changes under stress, and how the vibrational frequency is affected by these changes. Molecular vibrations are often approximated by a harmonic oscillator potential but, in reality, the molecular vibrations have a small anharmonic component[27]. For the harmonic potential, the force constant, k, does not change with distance so the vibrational frequency will be unaffected. For the anharmonic potential, however, the force constant is lowered slightly as the bond length increases with extensional stress on the molecule and, therefore, the vibrational frequency is reduced. Shifts in Raman frequency are not expected to be large unless the polymer molecules are extended; in the solid state, for example, the Raman shifts induced by uniaxial stress in crystalline polymer are much larger than in amorphous material. Hence, substantial shifts in Raman frequency are not expected for strain rates below $\dot{\epsilon}_c$.

Chain extended cPI is a linear molecule in which the double bonds are approximately parallel to the chain direction. In order to make a rough estimate of the effect of extensional flow on the frequency of the double bond, we have made the gross assumption that the polymer molecule can be represented by a linear row of beads connected by carbon double bonds.

The force required to increase the length R of a bond by δR is

$$f = k\delta R \tag{2}$$

where k is the bond stretching force constant. For this over-simplified model it is adequate to use an empirical relationship between force constant and the bond length. Badger's rule describes the anharmonicity of a bond in the form

$$k^{-\frac{1}{3}} = a_B(R - b_B) \tag{3}$$

where a_B and b_B are constants dependent upon the atoms bonded together[28]. The approximate shift in vibrational frequency of the bond is then given by[29]

$$\delta\nu \approx -\frac{3}{2}\frac{\nu}{(R - b_B)}\delta R \tag{4}$$

In this model, the force acting on each bond arises from the viscous interaction between the beads and the fluid in the extensional flow field. The relative velocity of the solvent with respect to the molecule increases from the centre of

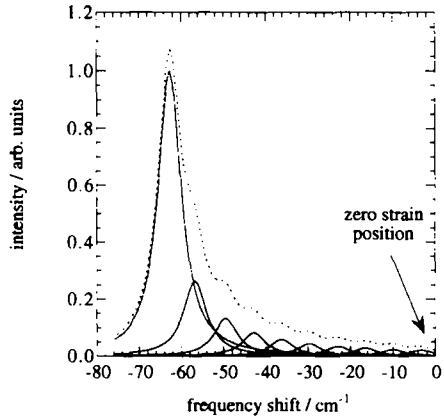

Figure 17 Prediction (dotted line) for the Raman band of the ν(C=C) vibration for a 0.05% solution of 4.4 × 10^6 M_w *cis*-polyisoprene in 1,1,1-trichloroethane at a strain rate of 8000 s^{-1}. The prediction is the summation of ten Lorentzians (solid lines) corresponding to the distribution of bond stresses shown in *Figure 16*

gravity of the chain outwards. The frictional forces caused by the contact with the fluid create tension in the chain with the maximum stress in the centre[30]. The force F_i on the ith bead from the centre can be calculated using Stokes Law as

$$F_i = 6\pi\eta a S v_{ri} \tag{5}$$

where a is the radius of the bead, η is the solution viscosity, S is a shielding factor which accounts for the effect that the beads have on each other[31] and v_{ri} is the relative velocity of the solvent compared to the ith bead. The total force on each bead $F_{i(\mathrm{tot})}$ is given by the sum of the forces acting on the beads from the end bead to the ith bead,

$$F_{i(\mathrm{tot})} = 3\pi\eta abS\dot{\epsilon}\left[\frac{N^2}{4} - i^2\right] \tag{6}$$

where b is the separation between beads, N is the total number of beads, v_{ri} has been replaced by $b\dot{\epsilon}$ and i is the bead number ($-N/2 \leq i \leq N/2$). The stress distribution is thus parabolic with the maximum stress at the centre of the chain.

For this simple bead-rod model, the dependence of Raman frequency of the central bond on the strain rate is given by

$$\delta\tilde{\nu}_i = -\frac{3}{2}\frac{\pi\nu abS}{k(R - b_B)}\left[\frac{N^2}{4} - i^2\right]\eta\dot{\epsilon} \tag{7}$$

Thus the change of the Raman frequency in this simple model is proportional to strain rate, the viscosity of the solution and, through N, the square of the molecular weight.

The functional form of equation (7) is consistent with the observed experimental results. *Figures 8 and 9* show that, between $\dot{\epsilon}_c$ and $\dot{\epsilon}_s$, the Raman frequency decreases in direct proportion to $\dot{\epsilon}$. Furthermore, *Figure 15* shows that, for the solutions of concentration lower than 0.078%, the Raman frequency is proportional to the viscosity. We were, unfortunately, unable to obtain sufficiently good data to test the molecular weight dependence.

Rough estimates of absolute values for the changes in the Raman frequency for the central bond in the molecule were made using the following values in equation (7): $N = 58.27 \times 10^3$, $a = 1.46 \times 10^{-10}$ m, $b = 3.46 \times 10^{-10}$ m, $S = 0.2037$ (from Ref. [31]), $b_B = 0.68 \times 10^{-10}$ m and $R = 1.37 \times 10^{-10}$ m. For the 0.05% and 0.087% cPI solutions at $\dot{\epsilon} = 8000\ \mathrm{s}^{-1}$, the predicted values are 50 cm^{-1} and 65 cm^{-1}, respectively.

The parabolic distribution of stress along the bonds of a polymer chain calculated using the bead-rod model is shown in *Figure 16*(a). The distribution has been normalised to make the maximum stress and bond number both equal to 1. The relative number of bonds in each stress interval is shown in *Figure 16*(b); it can clearly be seen that the number of bonds in the stress interval is largest at the highest stress. In order to predict the expected shape for the Raman band, the curve in *Figure 15*(b) was split into 10 bands. A Lorentzian curve was calculated for each band with intensity proportional to the number of bonds in that stress band. The widths of all the Lorentzian curves were fixed at 5 units and the curves were spaced 10 units apart. Therefore, the expected shape of the Raman band is approximately that of the sum of the ten Lorentzian curves as is shown in *Figure 17*. This graph shows that a dramatic shift in frequency towards the maximum bond stress position is expected, as the number of the bonds in this strain interval is the greatest. The Raman band is also expected to have an asymmetric tail to the zero strain position. Thus, because the maximum calculated Raman shift for a 0.087% cPI solution at $\dot{\epsilon} = 8000\ \mathrm{s}^{-1}$ is 65 cm^{-1}, the maximum of the expected Raman band will occur at approximately this frequency.

The changes observed for the Raman frequency in the region of extensional flow are much less than the calculated values. In the previous example of a 0.087% solution, the calculated frequency shift is 65 cm^{-1} but the measured shift for that solution was only 1.3 cm^{-1}: for a 0.05% solution, the predicted shift was 50 cm^{-1} but the observed shift was only 0.5 cm^{-1}, 100 times smaller. This disagreement is a strong indication that the Raman spectra are not typical of fully or even partially extended polymer molecules.

Molecular structure in the extensional flow field

The evidence from the birefringence, Rayleigh scattering and Raman depolarisation studies is that the polymer molecules have a high degree of alignment in the direction of the extensional flow field. These results cannot be used, however, to discriminate between local alignment of chain segments and a high degree of extension of the polymer molecules. There are two experimental results that can, in principle, be used to make that discrimination. The molecular scission results of Odell *et al.*[2] provide very strong evidence for mid-chain rupture at high values of $\dot{\epsilon}$; this is very difficult to understand if the molecules are not in a highly extended state. The other experiment that can make that discrimination is the present one. The Raman results presented here give a very strong indication that the molecules are far from being fully extended. Even if the force model developed above is oversimplified, experimental results on polydiacetylene single crystals indicate that a ν(C=C) vibration frequency should shift by at least 100 cm^{-1} before fracture of the polymer chain could occur[32].

Hence, it is very difficult to reconcile the results of the present experiments with those of chain scission experiments. It has been suggested that the Raman measurements are suspect because of screening effects caused by insufficient dilution[6]. As discussed above, however, the solutions appear to be well-behaved for $\dot{\epsilon} < \dot{\epsilon}_s$. Furthermore, some of the results used to demonstrate molecular scission were carried out[2] using solutions, e.g. a 0.1% solution of 1.4 × 10^6 M_w polyethylene oxide in water, that would now be regarded as having a sufficiently high concentration to show screening effects[6].

It is possible, however, that the two contradictory

experiments can still be reconciled. The signal levels in the present Raman experiments are too low to detect a group of chain-extended molecules if they represented less than about 10% of the total number of solute molecules. The presence of such a group, even though a small fraction of the total, might be sufficient to explain the chain scission results. There has been considerable discussion about the fraction of molecules in the region of extensional flow that experience scission[8]. The Raman experiments still challenge, however, the long-held view that the birefringence in the region of extensional flow arises largely from highly extended polymer molecules.

The present experimental observations strongly indicate that the majority of the polymer molecules do not stretch out fully even though there is a substantial degree of molecular alignment with the flow field. This could occur if the molecules instead remain in a 'folded', 'kinked' or 'multi-stranded yoyo' state[9]. The rheological behaviour of the bead-rod model was calculated by Acierno who discovered that some of the chains do not fully extend in the flow but end up folded in parts[33]. Simulations of a freely jointed chain by Rallison and Hinch showed similar results[34]. Brownian dynamics simulations of polymer chains have also shown that molecules are driven into a 'kinked' state by the flow field[35]. The number of folds in the molecule decreases with increasing residence time of the molecule in the flow field.

The calculated force at the centre of the chain is related to the square of the length of the chain. If there are kinks or 'back loops' present in the chain the tensile force at these must tend to zero[35] and, therefore, the 'free length' of the chain over which strain can accumulate will be concomitantly reduced. As the tension in the chain depends on the dimension of the stretched segment of the chain[36], so the expected frequency shifts will also decrease.

The changes in the expected frequency shift based on the number of folded segments has been estimated. To simplify the calculation, it was assumed that the folded segments all had the same length and the strain was zero at the kink points. The Raman shift was calculated for the centre bond in each of the segments because, as shown earlier, the observed frequency shift tends to that value. The force on this bond was calculated by assuming that the effective number of beads in each folded segment was N/f where f is the number of segments. The expected Raman shift drops rapidly with increasing number of segments; therefore, there need only be a few folds remaining in the molecule for the observed Raman shift to be radically reduced.

If the molecule remains in a folded state this may affect the force required to stretch the molecule. The extensional flow field will not be able to transfer as much force to the molecule because the inner beads will be shielded from the flow by the outer ones and the surface for viscous drag will be reduced. This can be modelled by assuming that the effective bond force constant for the C=C bond becomes larger by a factor of f. The frequency shift for this model tends to zero rapidly with increasing number of folds; for $f = 3$ the expected shift is reduced to 3 cm^{-1}.

Although the kinks model gives a potential explanation for the Raman data, it is contradicted by the observed phenomenon of chain halving above the critical strain rate for chain scission. If the molecules are driven into a folded state the maximum stress may not occur at the exact centre of the chain as has been observed experimentally[2]. Furthermore, mechanical degradation of chains requires high strains to be present along the chain regardless of the model used; therefore large Raman shifts are expected at the strain rate wherever chain scission occurs. In addition, the extensional flow field used in the calculation of the kinked state by Rallison and Hinch[34] was considerably stronger than that used in the present experiments. For these reasons, the kinks model, although giving a plausible explanation for the low Raman shifts may not be applicable to these experiments.

Hunkler *et al.* suggest (see figure 4 in Reference [9]) that, in transient extensional flow for $M_w < 4 \times 10^6$, the structure of the polymer is best described by a multi-stranded yo-yo while for $M_w > 4 \times 10^6$, the structure of the polymer in extensional flow with a stagnation point is best described by the extended chain[9]. The authors suggest that there is insufficient data for a description of the polymer chain in the two other regions. The present Raman measurements have been carried out for polymer chains of $M_w \leq 4 \times 10^6$ for extensional flow with a stagnation point. In this region the Raman data strongly suggest that the polymer molecules do not approach full extension even though a high degree of molecular alignment is observed. A multi-stranded yo-yo model with the number of strands typically between three and five might provide the best explanation for the present data.

SCREENING EFFECTS

For a number of years it was believed that a solution could be regarded as 'dilute' in extensional flow studies provided that the concentration of the solution was below c^* [1]; the data supporting this belief came primarily from spatially unresolved birefringence measurements and laser Doppler velocimetry. In this context, the term dilute was taken to mean that the behaviour of a particular polymer chain is unaffected by the dynamics of neighbouring chains; alternatively, the concentration is sufficiently low for the coil-stretch transition not to perturb the flow field. The recent spatially resolved birefringence results of Carrington *et al.*[6] suggest, however, that screening effects occur at much lower concentrations than c^*. To be truly dilute it was suggested that the solution concentration must be as low as $c^*/100$. In the present experiments, the observation of saturation effects in Rayleigh scattering and Raman band depolarisation ratio, as well as in the frequency shift of the Raman band, appear to be strongly analogous to that observed in spatially resolved birefringence results with solutions in the concentration range $c^*/10 < c < c^*$.

Raman spectroscopy of solutions in which screening is relatively unimportant is possible in principle. Resonance Raman spectroscopy of polymer solutions has been carried out with concentrations well below 0.001%[37]. This has only been possible thus far, however, with conjugated polymers that are too rigid to be affected by an extensional flow field[38]. Resonance Raman scattering with polymers having coil-rod extensibility could be achieved, in principle, with an ABA tri-block co-polymer. The A blocks should be synthesised from a flexible polymer with high molecular weight, and roughly equal length, such as atactic polystyrene. The central B block, perhaps 50–100 repeat units, should be a conjugated polymer with strong resonance Raman scattering. The B block would then act as a Raman strain gauge[39] at the centre of the polymer chain where the stress should be greatest.

CONCLUSIONS

In this paper the application of Raman spectroscopy to extensional flow experiments has been reported. The optical

configuration enabled spectra to be obtained with a spatial resolution of 10 μm in the region of extensional flow. This direct measurement in a small scattering volume represents an advantage over the technique of birefringence measurement which requires the use of deconvolution formulae to recover the spatial distribution of strain. The frequency, intensity and depolarisation ratio of the Raman band associated with the double bond vibration of *cis*-polyisoprene were measured.

No changes were observed in the Raman spectra until the strain rate was larger than the critical value. The vibrational frequency was then observed to decrease linearly with increasing strain rate until, at sufficiently high strain rate, the frequency saturated. The saturation effect has been associated with distortion of the flow field caused by molecular stretching. Between the onset and saturation of the Raman shift, the intensity of the Raman band was observed to increase and the depolarisation ratio to decrease; both of these measurements indicated an increasing degree of molecular orientation along the symmetry axis of flow. The observed changes in the Raman frequency were, however, about 1% of those predicted using a model of a fully extended chain in the flow field. These results together suggest that the majority of polymer molecules were not highly extended even though there was a high degree of molecular alignment. The Raman experiments thus challenge the view that the birefringence in the region of extensional flow arises primarily from highly extended polymer molecules.

ACKNOWLEDGEMENTS

The authors are indebted to Dr J. A. Odell for the inspiration to carry out this work and for giving generously of his knowledge and experience of extensional flow. The project was supported by the SERC.

REFERENCES

1. Keller, A. and Odell, J. A., *Colloid Polym. Sci.*, 1985, **263**, 181.
2. Odell, J. A., Keller, A. and Müller, A., *J. Colloid Polym. Sci.*, 1992, **270**, 307.
3. Mackley, M. R. and Keller, A., *Phil. Trans. R. Soc. A*, 1975, **278**, 29.
4. Frank, F. C. and Mackley, M. R., *J. Polym. Sci. B*, 1976, **14**, 1121.
5. Cathey, C. A. and Fuller, G. G., *J. Non-Newtonian Fluid Mech.*, 1990, **34**, 63.
6. Carrington, S. P., Tatham, J. P., Sáez, A. E. and Odell, J. A., *Polymer*, 1997, **38**, 4151.
7. Carrington, S. P., Tatham, J. P., Sáez, A. E. and Odell, J. A., *Polymer*, 1997, **38**, 4595.
8. Hunkler, D., Nguyen, T. Q. and Kausch, H. H., *Polymer*, 1996, **37**, 4257.
9. Hunkler, D., Nguyen, T. Q. and Kausch, H. H., *Polymer*, 1996, **37**, 4271.
10. Pope, D. P. and Keller, A., *Colloid Polym. Sci.*, 1978, **255**, 633.
11. Zimm, B. H., *J. Chem. Phys.*, 1956, **24**, 269.
12. De Gennes, P. G., *J. Chem. Phys.*, 1974, **60**, 5030.
13. Lopez Cascales, J. J. and Garcia de la Torre, J., *J. Chem. Phys.*, 1991, **95**, 9384.
14. Carl, W. and de Pablo, J. J., *Macromol. Theory Simul.*, 1994, **3**, 177.
15. Tatham, J. P., Extensional flow dynamics of macromolecules of different flexibility in solution. PhD thesis, University of Bristol, 1993.
16. Siesler, H. W., *Adv. Polym. Sci.*, 1984, **65**, 1.
17. Pearson, D. S., Kiss, A. D., Fetters, L. J. and Doi, M., *J. Rheol.*, 1989, **33**, 517.
18. Cornell, S. W. and Koenig, J. L., *Macromol.*, 1969, **2**, 546.
19. Brown, W. and Mortensen, K., *Macromol.*, 1988, **21**, 420.
20. J. Brandrup and E. H. Immergut (eds), *Polymer Handbook*, 3rd edn. Wiley Interscience, New York, 1989.
21. Press, W. H., Teukolsky S. A., Vetterling W. T. and Flannery B. P., *Numerical Recipes in FORTRAN*. Cambridge University Press, Cambridge, 1992.
22. Odell, J. A., Müller, A. J. and Keller, A., *Polymer*, 1988, **29**, 1179.
23. Menasveta, M. J. and Hoagland, D. A., *Macromolecules*, 1991, **24**, 3427.
24. Nyburg, S. C., *Acta Cryst.*, 1954, **7**, 385.
25. Chow, A., Keller, A., Müller, A. J. and Odell, J. A., *Macromol.*, 1988, **21**, 250.
26. Harlen, O. G., Hinch, E. J. and Rallison, J. M., *J. Non-Newtonian Fluid Mech.*, 1992, **44**, 229.
27. Tashiro, K., Wu, G. and Kobayashi, M., *J. Polym. Sci. B*, 1990, **28**, 2527.
28. Badger, R. M., *J. Chem. Phys.*, 1934, **2**, 128.
29. Mitra, V. J., Risen, W. M. and Baughman, R. H., *J. Chem. Phys.*, 1977, **66**, 2731.
30. Odell, J. A. and Keller, A., *J. Polym. Sci.*, 1889, **B 1986**, 24.
31. Feng, S. S., MacDonald, R. C. and Abraham, B. M., *J. Rheol.*, 1991, **35**, 565.
32. Batchelder, D. N. and Bloor, D., *J. Phys. C: Solid St. Phys.*, 1979, **17**, 569.
33. Acierno, D., Titomanlio, G. and Marrucci, G., *J. Polym. Sci. Polym. Phys. Ed.*, 1974, **12**, 2177.
34. Rallison, J. M. and Hinch, E. J., *J. Non-Newtonian Fluid Mech.*, 1988, **29**, 37.
35. Larson, R. G., *Rheol. Acta*, 1990, **29**, 371.
36. Rabin, Y., *J. Chem. Phys.*, 1987, **86**, 5215.
37. Taylor, M. A., Odell, J. A., Batchelder, D. N. and Campbell, A. J., *Polymer*, 1990, **31**, 1116.
38. Taylor, M. A., Batchelder, D. N. and Odell, J. A., *Polymer*, 1988, **29**, 253.
39. Robinson, I. M., Young, R. J., Galiotis, C. and Batchelder, D. N., *Proceedings of the Sixth International Conference on Composite Materials*, Vol. 1, eds. F. L. Matthews, N. C. R. Buskell, J. M. Hodgkinson and J. Morton. Elsevier Applied Science, London, 1987, p. 333.